AIMS Materials Science, 3(1): 66-82.
DOI: 10.3934/matersci.2016.1.66
Received: 12 November 2015
Accepted: 10 January 2016
Published: 12 January 2016

http://www.aimspress.com/journal/Materials

Research article

Fluidity of biodegradable substrate regulates carcinoma cell behavior: A novel approach to cancer therapy

Sharmy S Mano [1], Koichiro Uto [1,2], Takao Aoyagi [1], and Mitsuhiro Ebara [1,*]

[1] Smart Biomaterials Group, Biomaterials Unit, International Center for Materials Nanoarchitectonics (WPI-MANA), National Institute for Materials Science (NIMS), 1-1 Namiki, Tsukuba, Ibaraki 305-0044, Japan

[2] Present Address: Department of Bioengineering, University of Washington, 3720 15th Ave NE, Seattle, WA 98195, United States

* **Correspondence:** Email: EBARA.Mitsuhiro@nims.go.jp; Tel: +81-29-860-4775; Fax: +81-29-860-4708.

Abstract: Although various polymeric substrates with different stiffness have been applied for the regulation of cells' fate, little attention has been given to the effects of substrates' fluidity. Here, we implement for the first time biodegradable polymer with fluidic property for cancer therapy by investigating cell adhesion, proliferation, apoptosis/death, cycles of cancer cells as well as the anticancer drug efficacy. To achieve this, we prepared crosslinked and non-crosslinked copolymers of ε-caprolactone-*co*-D, L-lactide (P(CL-*co*-DLLA)). The tensile test showed the crosslinked P(CL-*co*-DLLA) substrate has the stiffness of 261 kPa while the loss modulus *G"* of the non-crosslinked substrate is always higher than the storage modulus *G'* (*G"*/*G'*=3.06), indicating a quasi-liquid state. Human lung epithelial adenocarcinoma cells on crosslinked substrate showed well- spread actin stress fibers and visible focal adhesion with an increased S phase (decreased G0/G1 phase). The cells on non-crosslinked substrate, on the other hand, showed rounded morphology without visible focal adhesion and an accumulated G0/G1 phase (decreased S phase). These results suggest that the behavior of cancer cells not only depends on stiffness but also the fluidity of P(CL-*co*-DLLA) substrate. In addition, the effects of substrate's fluidity on anti-cancer drug efficacy were also investigated. The IC_{50} values of paclitaxel for cancer cells on crosslinked and non-crosslinked substrates are 5.46 and 2.86 nM, respectively. These results clearly indicate that the fluidity of polymeric materials should be considered as one of the crucial factors to study cellular functions and molecular mechanism of cancer progression.

Keywords: fluidity; poly (ε-caprolactone); cancer cells; cell cycle; paclitaxel

1. Introduction

Extracellular matrix (ECM) provides both mechanical and biochemical supports to cells and cellular activities are greatly influenced by the surrounding environments [1–5]. Indeed, abnormal ECM associated with the formation and development of diseases like cancer [6]. The biophysical and biochemical cues from tumor-associated ECM, for example, influence cancer properties such as malignancy [7]. Tumors are instinctively stiffer than the surrounding normal tissues. Researches show that ECM conjugated synthetic hydrogels of a variety of stiffness control the migration and properties of cancer cells by regulating cellular behavior [8–11]. A recent study reveals that 3D soft fibrin gels promote the selection and differentiation of tumor cells from cancer cells [12].

While biomaterials research field have recently focused on the micromechanical properties of a scaffold [13,14], it is yet unclear how the mechanical properties of widely used biodegradable polymers influence cell behavior. Biodegradable polymers conjugated with nanoparticles have been used in drug delivery systems for the treatment of cancer for many years [15,16]. For example, dexamethasone encapsulated on amphiphilic block copolymers containing polyethylene glycol (PEG) and poly (ε-caprolactone) (PCL) were induce the death of pediatric leukemia cells [17]. Paclitaxel conjugated with superparamagnetic iron oxide (SPIO) loaded on poly (lactic-*co*-glycolic acid) (PLGA) based nanoparticles are effective for the imaging and therapy of murine colorectal carcinoma CT26 cells in vitro and in vivo [18]. Cancer therapies by biodegradable materials, however, are under surveillance for the treatment of wide range of cancer targets because the effects of mechanical properties of biodegradable polymers on cancer progression and anti-cancer drug efficacy are not yet clear. Especially, the effects of substrate fluidity are poorly understood.

From this regard, we have been developing semi-crystalline PCL substrates with different elasticity and topography but similar surface wettability. PCL is an important class of the biocompatible and biodegradable synthetic polymers [19], which is approved by the food and drug administration (FDA) for biomedical applications [20,21]. We have demonstrated that the mechanical properties of PCL can be controlled by adjusting the amorphous-crystal phase transition temperature (T_m) [22]. In this study, we prepared fluidic substrate by copolymerizing CL with D, L-lactide (DLLA). The T_m was successfully adjusted below 37^{o}C; *i.e.* the P(CL-*co*-DLLA) displays liquid-like behavior at 37 ^{o}C. Moreover, the fluidity was controlled by chemically crosslinking the functionalized end chains of P(CL-*co*-DLLA). To understand the effects of substrate fluidity on the behavior of cancer cells, we cultured human lung epithelial adenocarcinoma cells on the crosslinked and non-crosslinked P(CL-*co*-DLLA) substrates and observed cell morphology, focal adhesion, proliferation, cell death and cell cycle (Figure 1). Furthermore, the effects of substrate's fluidity on anti-cancer drug efficacy were investigated using paclitaxel. The IC_{50} values for cancer cells on crosslinked and non-crosslinked substrates were examined and which depends on the growth profile of cancer cells on P(CL-*co*-DLLA) substrate.

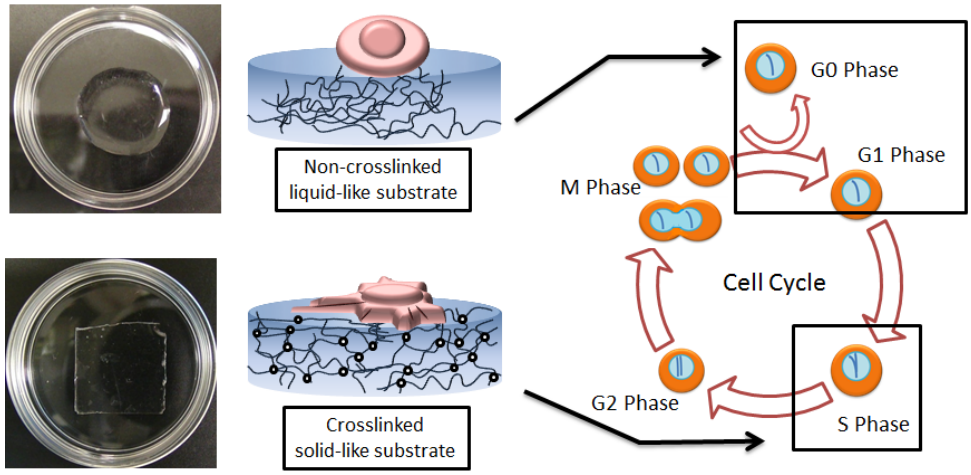

Figure 1. Schematic illustration of adhesion, spreading behavior and phases of cell cycle (highlighted by squares) of NCI-H23 cells on crosslinked and non-crosslinked P(CL-*co*-DLLA) substrates. Cells on non-crosslinked (liquid-like) substrates are rounded in morphology with less cell spreading area and an accumulated G0 (resting phase) or G1 phase (gap phase) (upper figure) and cells on crosslinked (solid-like) substrates are well spread and accumulated in S phase (synthesis phase) (lower figure) of cell cycle.

2. Materials and Method

2.1. Preparation of non-crosslinked substrate

Four-branched copolymers of ε-caprolactone were synthesized according to our previous reports [23,24]. The structure and molecular weights were estimated by ^{1}H NMR spectroscopy (JEOL, Tokyo, Japan) and gel permeation chromatography (GPC; JASCO International, Tokyo, Japan) respectively. The viscoelastic properties of non-crosslinked PCL substrates were tested using a rheometer (MCR 301, Anton Paar, Tokyo, Japan) with parallel plate geometry (rotating top plate of 10 mm diameter). The viscoelastic spectrum (storage modulus, G' and loss modulus, G'') as a function of frequency and temperature were measured.

For cell culture experiment, P(CL-*co*-DLLA) was dissolved in toluene at 80 wt %. The prepared P(CL-*co*-DLLA) was then spin coated on glass coverslips of 24 well insert (15mm) or 6 well insert (35mm) as per the requirement of the experiments, at 15000 rpm for 1 minute. Prior to cell culture, the substrates were sterilized by low pressure hydrogen peroxide gas plasma system CH-160C (Toho Seisakusho, Tokyo, Japan) and equilibrated with Roswell park memorial institute 1640 (RPMI 1640; Nacalai Tesque, Kyoto, Japan) medium for 1 h followed by one time washing with phosphate buffered saline (PBS).

2.2. Preparation of crosslinked substrate

The crosslinked P(CL-*co*-DLLA) substrate was prepared by according to previous reports [23,24]. The mechanical property of the crosslinked substrate was characterized by a tensile test (EZ-S 500N; Shimadzu). For cell culture experiment, the crosslinked substrate was cut into the

size of 24 well inset or 6 well insert.

2.3. Cell culture

Human lung epithelial adenocarcinoma cells (NCI-H23; ATCC) were cultured in RPMI supplemented with 10% heat-inactivated fetal bovine serum (FBS; ATCC), 1% antibiotic-antimycotic (anti-anti, Gibco, Grand Island, NY, USA), MEM non-essential amino acids (Gibco) and sodium pyruvate (Gibco). The cells were maintained at 37°C under humidified atmosphere of 5% CO_2.

2.4. Cell proliferation and adhesion assay

For proliferation assay, NCI-H23 cells were seeded on glass coverslip or P(CL-*co*-DLLA) (crosslinked and non-crosslinked) substrates of 24 well plate inserts at a density of 10000 cells/well. The cells were incubated at different time periods such as 1, 2, 3 and 5 days. The cell proliferation assay was performed with CyQuant® NF cell proliferation assay kit (Invitrogen) according to the manufacturer's instructions. Cell adhesion assay was performed for 6 h and total cell number was determined using CyQuant® NF cell proliferation assay kit. Percentage of cell adhered on glass substrate were calculated from the initial cell seeding and the relative cell adhesion were determined by compared to cells on glass substrate.

2.5. Immunostaining and confocal microscopy

For confocal microscopy, 10000 cells were seeded on glass coverslip or P(CL-*co*-DLLA) (crosslinked and non-crosslinked) substrates and incubated for one day. The cells were fixed by 4% paraformaldehyde (PFA; Wako, Japan) and blocked by 1% bovine serum albumin (BSA; Sigma-Aldrich) (in PBS) for 30 min and stain with monoclonal anti-vinculin antibody (1:200; Sigma-Aldrich), and the corresponding secondary antibody (1:100; Alexa Fluor® 488 anti-mouse antibody, Invitrogen) for 1 h each. F-actin and nuclei were stained by tetramethylrhodamine B isothiocyanate-conjugated phalloidin (Sigma-Aldrich) and 4',6-diamidino-2-phenylindole (DAPI; Sigma-Aldrich) respectively. The cells were observed and the images were taken by Leica SP5 confocal laser scanning microscope (Leica, Wetzlar, Germany). The nuclear shape index (NSI) was measured by ImageJ (Rasband, W.S., National Institutes of Health, Bethesda, Maryland, USA) from the relationship: $NSI = 4\pi \times area/(perimeter)^2$ [25].

2.6. Apoptosis and dead cell assay

5×10^5 cells/well were seeded on glass coverslip or P(CL-*co*-DLLA) (crosslinked and non-crosslinked) substrates of 6 well inserts and incubated. After 3 days, cells were stained by FITC Annexin V/Dead Cell Apoptosis Kit with FITC annexin V and PI, for Flow Cytometry (Invitrogen) according to the manufacturer's instructions. The percentage of apoptosis and dead cells were measured by analyzing the cells with spectral cell analyzer (LE-SP6800A, Sony, Japan). 10000 cells were analyzed for each sample.

2.7. Cell cycle analysis

Cells were grown on culture medium contains 10% serum in 100mm dishes. After attaining 80–100% of confluence, 5×10^5 cells/mL were cultured on 6 well plates in serum free medium to synchronize the cells in G0/G1 phases of cells cycles. To optimize the condition for cell cycle synchronization, cells were incubated for 18, 20, 24, 48 and 72 h. Cells cultured on 10% serum containing medium was maintained as a control. After the above-mentioned incubation, cells were harvested and fixed by 1mL of 70% ethanol (in PBS) overnight at 4 °C. The cells were stained by FxCycle^{TM} PI/RNase staining solution (Invitrogen) for 30 minutes according to the manufacture's instruction. Then the cells were analyzed by spectral cell analyzer (LE-SP6800A, Sony, Japan) and the percentage of each phase of the cell cycle was analyzed by ModFit LT4.1 software (Verity software). Synchronized cells were seeded on glass coverslip or P(CL-*co*-DLLA) (crosslinked and non-crosslinked) substrates of 6 well inserts at the density of 5×10^5 cells/mL for 6, 18, 24, 48 and 72 h in the cell culture medium contains 10% serum. The release of the cell cycle was analyzed as described above. Cell cycles were also monitored after 3 days of culture on glass coverslip or P(CL-*co*-DLLA) (crosslinked and non-crosslinked) substrates.

2.8. Anti-cancer activity

For anti-cancer drug activity, the cells were seeded at a density of 10000 cells/well on glass coverslip or P(CL-*co*-DLLA) (crosslinked and non-crosslinked) substrates of 24 well plate inserts and incubated for one day. After incubation, the cells were exposed by different concentration (0.1–50 nM) of paclitaxel (Taxol, Sigma-Aldrich) and continued the incubation one more day. The anticancer activity of the drug was estimated by analyzing the cell proliferation using CyQuant NF proliferation assay kit as described before (see section 2.4). Half maximal inhibitory concentration (IC_{50}) of paclitaxel for 50% of cell survival was calculated by using GraphPad Prism 6 (GraphPad Prism Software).

2.9. Statistical analysis

All results were represented as mean ± standard deviation (SD) obtained from three independent experiments. The degree of significance of each data was analyzed by Student's t-test by compared with glass or P(CL-*co*-DLLA) (crosslinked and non-crosslinked) substrates or control group. Where, $p < 0.05$ is considered as statistically significant.

3. Results

3.1. Characterizations of crosslinked and non-crosslinked substrates

In our earlier studies, novel techniques to control the melting temperature (*Tm*) of PCL have been reported by tailoring the number of branched chains [23,24] for biological applications [26,27]. As an alternative approach, we also reported that *Tm* was adjusted below human body temperature by copolymerization of different ratios of CL with DLLA [28]. In this study, four-branched copolymers with CL/DLLA ratio of 60/40 were synthesized by ring-opening polymerization from

pentaerythritol. The obtained copolymers were then reacted with acryloyl chloride to introduce vinyl groups at the end chains. The molecular weight (Mw) and molecular number (Mn) of copolymers are 59,600 and 40,900 respectively (Mw/Mn = 1.46) as determined by GPC. The CL and DLLA contents of the copolymers were determined by ^{1}H-NMR is 61.1 and 38.9 mol% respectively when the feed concentration was 60 and 40 mol%. These data showed that copolymers with the desired branch number, molecular weight, and composition of CL and DLLA have been obtained (see Supplementary data. Table S1). The T_m of P(CL-*co*-DLLA) was found at 40 ± 1 ^{o}C, whereas it disappeared after crosslinking. The viscoelastic properties of the non-crosslinked substrate are storage modulus, G' = 1.08 × 10^4 Pa, loss modulus, G'' = 3.30 × 10^4 Pa and tan δ (=G''/G') = 3.06 (>>1 means that the substrate is viscous materials). These data were measured at an angular frequency of 10 s^{-1} at 37 °C. The shear modulus (G*) of the non-crosslinked P(CL-*co*-DLLA) substrate is 34.7 kPa calculated from the formula √ (G')2 + (G")2. The tensile test showed the crosslinked P(CL-*co*-DLLA) substrate has the stiffness of 261 kPa.

3.2. Effects of substrate fluidity on cancer cell morphology

To know the effects of the fluidity of substrates on cancer cell morphology, cytoskeletal organization, and focal adhesion, NCI-H23 cells were cultured on crosslinked and non-crosslinked P(CL-*co*-DLLA) substrates for 24 h (Figure 2a). Cells cultured on glass coverslip were maintained as control (top images). NCI-H23 cells on crosslinked substrate spread well and showed a visible actin stress fibers (middle images). However, in the case of non-crosslinked substrate, the cells were rounded and have less cell spreading area with unorganized actin filament (bottom images). A similar result was also obtained at 6 h incubation (data not shown). To visualize focal adhesion protein in cell attachment, the cells were stained for focal adhesion protein vinculin. Cells on crosslinked P(CL-*co*-DLLA) substrate showed visible vinculin-positive focal adhesion (indicated by arrows), suggesting that the cells were attached on crosslinked substrate by focal adhesion molecule. However, the cells on non-crosslinked substrate showed no vinculin-positive focal adhesion. The adherent cell morphology also influences the shape of the nucleus. To understand this phenomenon, NSI was measured (Figure 2b). The NSI of cells on glass and crosslinked P(CL-*co*-DLLA) substrates are 0.72 and 0.75 respectively. However, in the case of non-crosslinked P(CL-*co*-DLLA) substrate, NSI is significantly increased to 0.87. This result suggests that the rounded morphology of cell shape on non-crosslinked P(CL-*co*-DLLA) substrate influences the change in the nuclear shape of cells.

3.3. Effects of substrate fluidity on cancer cell proliferation

To understand the effects of crosslinked and non-crosslinked P(CL-*co*-DLLA) substrates on NCI-H23 proliferation, the cells were allowed to grow for 1, 2, 3 and 5 days. After the desired incubation periods, cell proliferation assay was performed independently. The proliferation rate of NCI-H23 cells on crosslinked substrate increased with increase the incubation time. The proliferation of NCI-H23 cells on non-crosslinked substrates was increased for day 1 and 2. On day 3 and 5, however, the cell proliferation rate was significantly reduced compared to glass or crosslinked P(CL-*co*-DLLA) substrates (Figure 3).

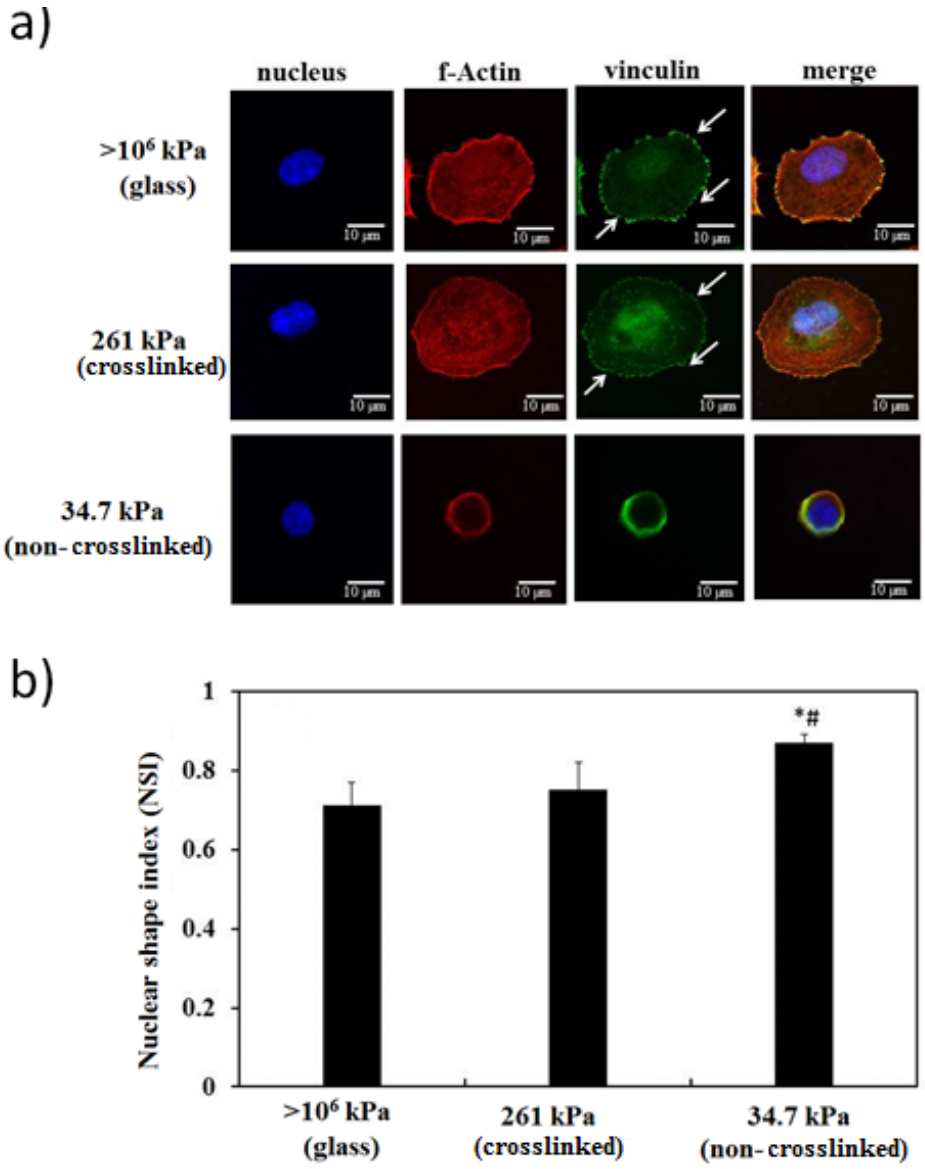

Figure 2. a). Morphology, cytoskeletal organization and focal adhesion of NCI-H23 cells on glass (>10^6 kPa), crosslinked (261 kPa) or non-crosslinked (34.7 kPa) P(CL-*co*-DLLA) substrates for 24 h. The cells were stained for nuclei (blue), F-actin (red) and focal adhesion protein vinculin (green). Cells on glass and crosslinked P(CL-*co*-DLLA) substrate showed a well-organized cytoskeletal arrangement and a well expressed focal adhesion protein vinculin (indicated by arrows). However, the cells on non-crosslinked P(CL-*co*-DLLA) substrate showed an unorganized cytoskeleton, rounded morphology with no visible expression or absence of focal adhesion protein vinculin. b). Nuclear shape index (NSI) of NCI-H23 cells on glass, crosslinked or non-crosslinked P(CL-*co*-DLLA) substrates. N = 50 ± SD, *$p < 0.05$ compared to glass and #$p < 0.05$ compared to crosslinked substrate.

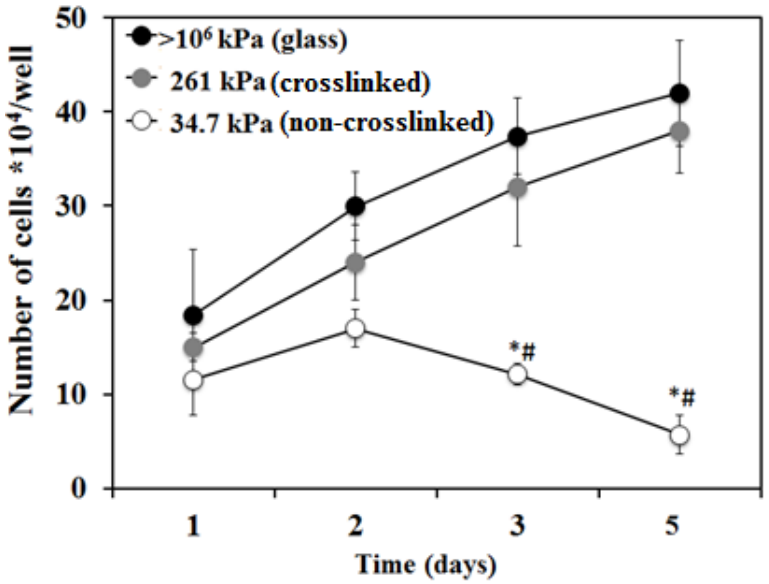

Figure 3. The proliferation of NCI-H23 cells on glass, crosslinked, and non-crosslinked P(CL-*co*-DLLA) substrates. NCI-H23 cells were cultured on glass (closed black circles), crosslinked (closed gray circles) or non-crosslinked (open circles) P(CL-*co*-DLLA) substrates for 1, 2, 3 and 5 days at 37 °C. Where, n = 3 ± SD, *p < 0.05 with respect to glass, #p < 0.05 with respect crosslinked substrate.

3.4. Effects of substrate fluidity on apoptosis and cycle of cancer cells

To understand the decrease in the proliferation of NCI-H23 cells on non-crosslinked P(CL-*co*-DLLA) substrates, possible reasons such as cell adhesion, cells apoptosis or cell death and or block in the phases of the cell cycle were examined. In order to know the percentage of cells adhered on the substrates; cell adhesion assay was performed at 6 h (Figure 4a). The relative adhesions of cells on crosslinked and non-crosslinked P(CL-*co*-DLLA) substrates are 94% and 82% respectively. To quantitatively monitor apoptotic and dead cell, apoptosis and dead cell assay were performed after 3 days of growth of NCI-H23 cells on glass, crosslinked or non-crosslinked P(CL-*co*-DLLA) substrates. Figure 4b shows a significant dead cell population (12.5%) on the non-crosslinked substrate while the cells do not exhibit significant apoptosis. To understand the effects of cell cycle on cell proliferation, the distribution of cells on different phases of cell cycle was also performed for 3 days of cell culture on the substrates (Figure 4c). Cells on crosslinked substrate showed a reduced G0/G1 phase and increased S phase. However, cells on non-crosslinked substrate showed a significant accumulation of G0/G1 phase and reduction of S phase. This suggested that there is a block in G1 phase that limited the leading of G1 to S phase. From the above findings, it was suggested that the difference in the cell proliferation on crosslinked and non-crosslinked P(CL-*co*-DLLA) substrates are attributed to the difference in of cell adhesion, cell death, and cell cycle.

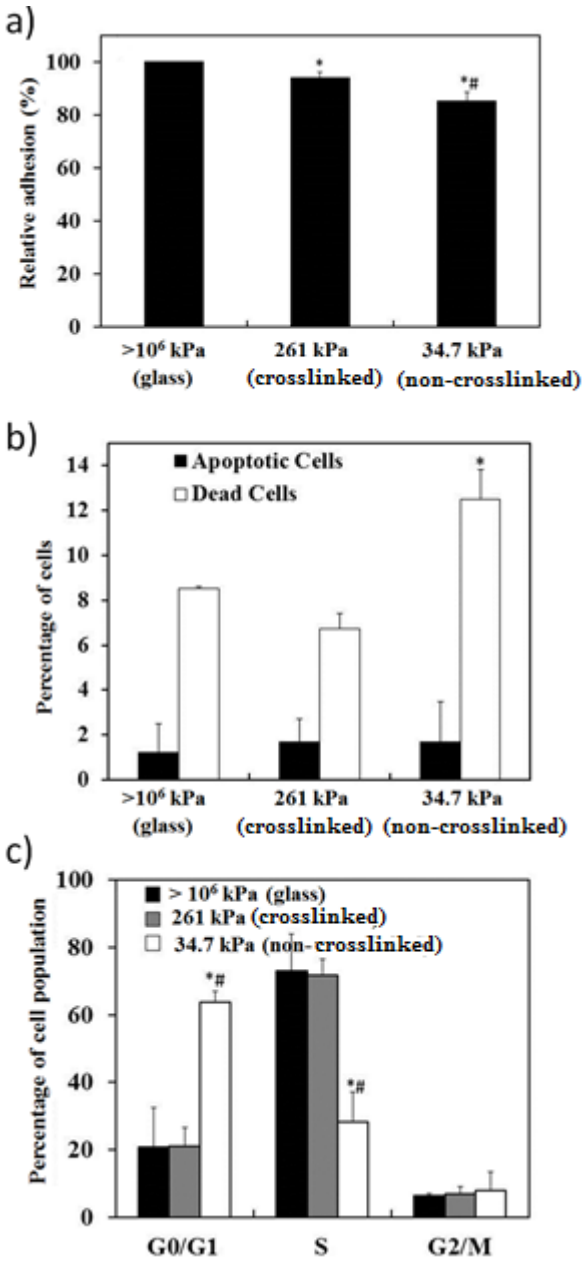

Figure 4. Effects of substrate fluidity on cell adhesion, cell apoptosis and death and cell cycle. NCI-H23 cells were cultured on glass, crosslinked or non-crosslinked P(CL-*co*-DLLA) substrate for 6 h or 3 days. a). The number of cell adhered were counted after 6 h of cell attachment. The percentage of cells adhered were calculated from the initial seeding density. Data were expressed as the relative percentage of cells adhered on the P(CL-*co*-DLLA) substrate by compared to glass. b). Percentage of apoptotic and dead cells were performed for 3 days of cell culture and c). Cell cycle was analyzed for 3 days of cell culture. n = 3 ± SD, *p < 0.05 with respect to glass and #p < 0.05 with respect to crosslinked substrate.

3.5. Cell cycle synchronization

Cell cycle synchronization is a key tool to understand cellular functions because cell behavior

and molecular mechanisms take place in the cells before cell division. From the above cell cycle result, it is known that crosslinked and non-crosslinked P(CL-*co*-DLLA) substrates have a greater influence on cell cycle that is reflected in the cell proliferation. To better understand the influence of substrate's fluidity on cell cycle, cells were synchronized at the G0/G1 phase and then cultured on the substrates. To achieve synchronization, cells were cultured on serum free medium and the percentages of cells in G0/G1 phase were monitored at different time periods such as 6, 18, 24, 48 and 72 h independently (Supplementary data Figure S1a). Cells were also cultured on 10% serum containing medium as a control. Control cells show 34.88% G0/G1 phase, 37.89% S phase and 27.23% G2/M phase. On the other hand, 42.7%, 52.8%, 73.8%, and 85.6% in G0/G1 phase were observed at 18 h, 20 h, 24 h, and 48 h of synchronization, respectively. Eventually, the cells were successfully synchronized to G0/G1 phase ((Figure 5a, red) at 72 h without S or G2/M phase. Although serum deprivation may induce the cells to become apoptotic, the percentage of apoptotic cells was determined. About 5.2% of the cells were found as apoptotic cells under serum deprivation (see Supplementary data Figure S1b).

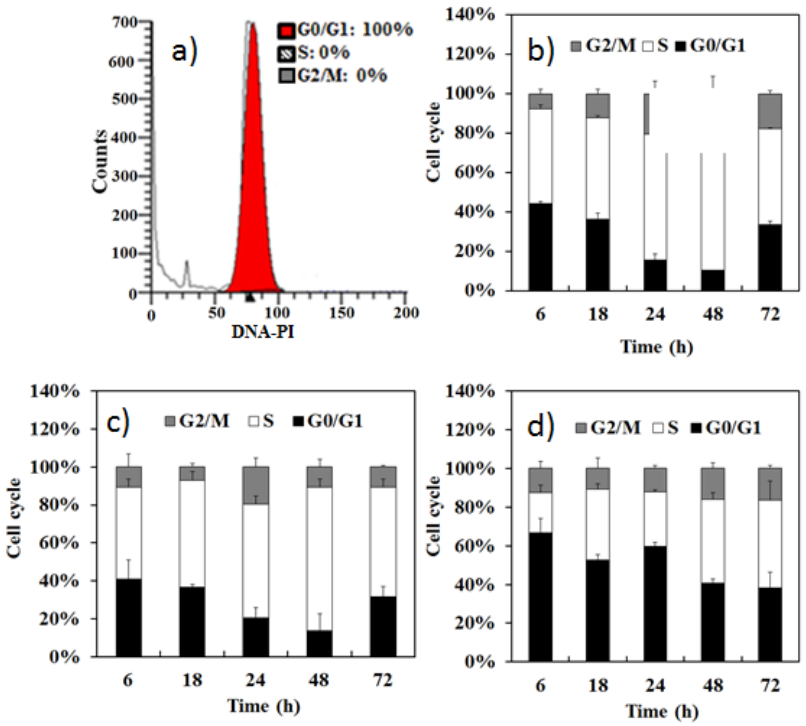

Figure 5. a). G0/G1 phase synchronized cells were cultured on 10% serum containing medium and analyzed the DNA content by propidium iodide (PI) staining a). at 0 h b). on glass c). on crosslinked and d) on non-crosslinked P(CL-*co*-DLLA) substrates and release of each phase of the cell cycle were monitored at 6, 18, 24, 48 and 72 h. Where, n = 3 ± SD, *p < 0.05 with respect to glass and #p < 0.05 with respect to the crosslinked P(CL-*co*-DLLA) substrate.

The G0/G1 phase synchronized cells were cultured on glass, crosslinked or non-crosslinked substrates in the presence of 10% serum containing medium (Figure 5). The influence of P(CL-*co*-DLLA) substrates on the release of each phase of the cell cycle were monitored for 6, 18,

24, 48 and 72 h (Supplementary data. Table S2). On glass substrate, cells entered into S phase and G2/M phase at 6 h (Figure 5b). At 18 h, the ratio of G0/G1 phase reduced and S phase increased with less G2/M phase distribution. At 24 h and 48 h, cells possess more G2/M phase than a G0/G1 phase. However, S phase was exponentially increased from 6h to 48 h and then reduced at 72 h. This showed that the cells demonstrated an uneven distribution of cell cycle with time on glass substrate. Cells on crosslinked P(CL-*co*-DLLA) substrates showed a slightly different image from cells on glass substrate (Figure 5c). When the cells were monitored from 6 to 48 h, cells possess an exponentially increasing S phase and decreasing G0/G1 phase with an unorganized distribution of G2/M phase. However, the cell cycle result is interestingly different for non-crosslinked P(CL-*co*-DLLA) substrates (Figure 5d). Cells in G0/G1 phase were gradually released to S phase with notable G2/M phase from 6 to 72 h. Thus, the non-crosslinked P(CL-*co*-DLLA) substrate is considered as an effective system to study the regulation of cell cycle.

3.6. Effects of anti-cancer drug on cancer cells on crosslinked and non-crosslinked substrates

To analyze the effect of anti-cancer drug paclitaxel, the cells were cultured on glass coverslip or P(CL-*co*-DLLA) substrates and exposed by paclitaxel at different concentrations from 0.1 nM to 50 nM. The cell number decreased with increase the concentration of paclitaxel from 0.1 nM to 50 nM (Figure 6a). The IC_{50} values of paclitaxel for NCI-H23 cells on glass, crosslinked and non-crosslinked P(CL-*co*-DLLA) substrates are 11.92 nM, 5.46 nM and 2.86 nM, respectively (Figure 6b). From this finding, it is suggested that low concentration of paclitaxel is enough to reduce the cell number to 50% on cells on the non-crosslinked P(CL-*co*-DLLA) substrate. This low concentration (2.86 nM) is statistically significant ($p < 0.05$) compared to IC50 of crosslinked P(CL-*co*-DLLA) substrate (5.46 nM).

4. Discussion

Natural polymers such as collagen, chitosan, elastin, and fibrinogen are used in the modeling of bioactive ECM analogs in tissue engineering [39]. On the other hand, biodegradable, synthetic polymers such as poly (glycolic acid), poly (lactic acid), poly (p-dioxanone) are used in tissue engineering and clinical applications [30]. Cell response to substrate rigidity is important to understand developmental morphogenesis and disease pathogenesis [31]. The stiffness of the matrixes plays a vital role in the regulation of cellular functions and stem cell differentiation. Mesenchymal stem cells (MSCs) grow on rigid matrix promotes the differentiation to smooth muscle cells (SMC) while softer matrix promotes its differentiation to chondrogenic and adipogenic lineage by regulating the expression of transforming growth factor β (TGF β) [32]. In the present study, we have established novel road for cancer therapy using PCL-based substrate. Especially, we demonstrated that the functions of cancer cells are regulated by not only elasticity but also the fluidity of the substrate.

Cancer cells on crosslinked (solid-like) substrate show well-spread cell morphology with an organized actin stress filament. However, cells on non-crosslinked (liquid-like) substrates possess circular morphology with unorganized actin filament without visible focal adhesion protein. This is due to the fact that the substrate in which the cell attached influences the change in cellular morphology [33]. Besides, the stiffness of the substrate could affect the structure of cells by

regulating the expression of alpha 5 integrin [34]. Cells adhere and interact with the substrate via transmembrane receptors called as integrins, which are connected intracellularly to the cytoskeleton through macromolecular protein assemblies known as focal adhesion. A recent study shows that rigidity of polyacrylamide (PA) gel regulates growth and morphology of cancer cells by regulating the formation of stress fibers and focal adhesion [35]. Indeed, focal adhesion plays a vital role in the regulation of cellular behaviors such as cell adhesion, migration, proliferation and differentiation [36].

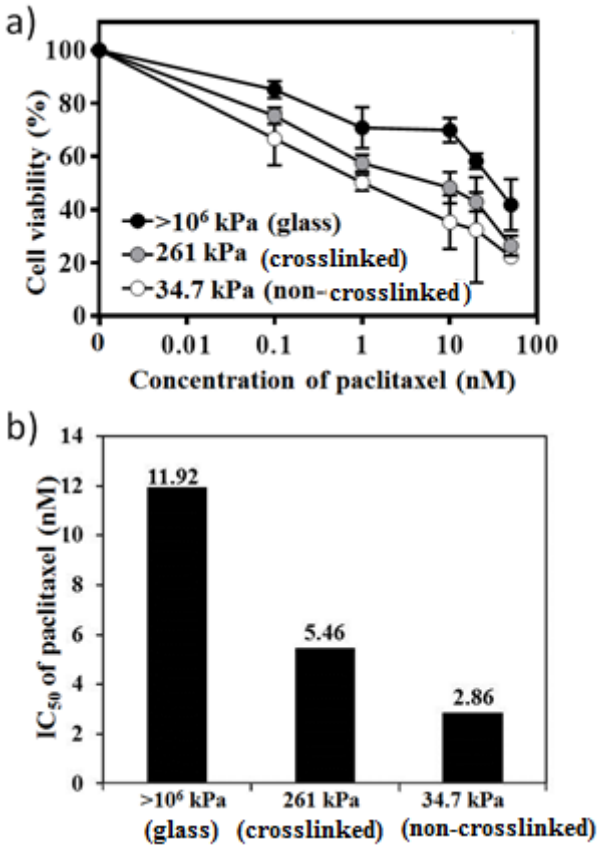

Figure 6. The dose-dependent activity of paclitaxel on NCI-H23 cells cultured on glass (closed circles) or crosslinked (closed gray circles) or non-crosslinked (open circles) P(CL-*co*-DLLA) substrates. NCI-H23 cells were exposed to paclitaxel at a concentration of 0.1 nM to 50 nM and cell number were monitored 24 h after paclitaxel exposure. b). IC_{50} value of paclitaxel was calculated from the dose-dependent activity. Where n=3±SD.

The morphology of the cell nucleus can be a powerful indicator of the condition of a cell as well as intent to identify its response to external stimuli. The change in the morphology influences the change in the nuclear shape [25]. NSI shows that cells on non-crosslinked substrate possess a slightly circular nucleus (NSI = 0.87) than the nucleus of the cells on crosslinked substrate (NSI = 0.75). The proliferation of NCI-H23 cells on the non-crosslinked substrate is reduced at longer incubation time (3 and 5 days) and percentage of cells adhered on the non-crosslinked substrate is less compared to cells adhered on crosslinked P(CL-*co*-DLLA) substrate. This suggests that low cell adhesion and proliferation is due to the lack of strong interaction between the cells and substrates. This is because

crosslinked and non-crosslinked P(CL-*co*-DLLA) substrates differ in their elasticity but possess similar surface wettability (crosslinked P(CL-*co*-DLLA) substrate: contact angle is 94.8 ± 3.7° and non-crosslinked P(CL-*co*-DLLA) substrate: contact angle is 94.6 ± 6.6°). From this regards, it is considered as fluidity and elasticity are the factors that regulate cellular adhesion and proliferation behavior of NCI-H23 cells on P(CL-*co*-DLLA) substrates.

Cell death is necessary for the physiological development of the organism and programmed cell death (PCD) is characterized as cell death by apoptosis, autophagy or senescence. A significant dead cell population was found on cells on non-crosslinked substrates but not apoptotic cell death. This suggests that cells may undergo non-apoptotic forms of PCD either by autophagy or by senescence [37]. Investigations are further needed to identify the reason for cell death on non-crosslinked substrates. Evidence shows that senescent human fibroblasts combat apoptosis stimulated by growth factor deprivation and oxidative stress [38]. Cell cycle results show that cells on non-crosslinked substrates have a predominant accumulation of G0/G1 phase with decreased S phase. Apoptosis cells largely distributed in S-phase, while growth arrested cells exhibited principally G1 and G2/M phase of cell cycle [39]. This indicates that the cells are not active owing to the decrease in the synthesis of key proteins needed for the promotion cell cycle [40] by the stress induced by the substrate in which the cells attached. In spite the fact that senescence types of cells possess flattened enlarged morphology and arrest in the G1 phase in response to stress [41]. However, the morphology of the cell on non-crosslinked P(CL-*co*-DLLA) substrate is rounded. This is due to the cells senses the fluidity of substrate surface and cell sensors at the membrane junction site signals for a relaxed rounded morphology [34].

Cell cycle synchronization is necessary to learn the biological properties, cellular functions, genetics and molecular regulatory mechanisms happen in cells prior to cell division. In cancer therapy, cell synchronization is used to identify several principal oncogenes and connected with specific cell cycle checkpoints [42]. There are several methods were adapted to synchronize the cell cycle at different phases [43] such as nutritional modulation [44], and also by using microchannels [45]. Here we employed serum deprivation method to induce cell cycle synchronization at G0/G1 phase [46]. Even-though, serum supplementation to culture medium is essential for the stimulation of growth and proliferation [47]. Serum deprivation induced the minimal amount of cells apoptosis. Cells on non-crosslinked substrate show an accumulated G0/G1 phase with a gradual release of S phase. This may be the fact that non-crosslinked substrate regulates the expression of cyclin D1 and retinoblastoma protein (Rb) phosphorylation necessary for S phase entry [48]. This indicates that the cells are not active and might be undergoing PCD as discussed above. While the cells on crosslinked substrate show an increased S phase in increased culture time. This gives a completely different picture on the behavior of cells on crosslinked and non-crosslinked substrates. Thus, the fluidity-tunable PCL-based substrate is considered as a suitable material to study the regulation of cancer behavior and molecular mechanism of cancer progression.

Paclitaxel is a well-known biopharmaceutics classification system (BCS) class IV drug which block the development of mitotic spindle fibers by binding with tubulin and effective against lung, ovarian, liver and ovarian cancer. Paclitaxel possesses poor solubility and poor permeability which serves to limit its oral uptake. In order to overcome such limitations, paclitaxel could be mixed with adjuvants like Cremofor-Ethanol (CrEL) and facilitate intravenous administration. On the other hand, hydrogels of agarose, poly (L- lactic acid) and chitosan-glycerolphosphate have been used to succeed crystallization of paclitaxel for effective drug delivery [49]. Intravenous administration of

nanosuspension of paclitaxel to xenograft mice increased its anti-cancer activity [50]. In the present study, paclitaxel shows a linear relationship to the death of the cells on crosslinked and non-crosslinked substrates. IC_{50} value for paclitaxel depends on the type of the cell and increasing the concentration over 50 nM does not enhance its cytotoxicity [51]. Cells on non-crosslinked substrate demonstrated that minimum paclitaxel concentration (2.86 nM) is enough to achieve IC_{50}.

In summary, crosslinked and non-crosslinked substrates play a vital role in the regulation of cancer cell behavior. Cell morphology and proliferation are greatly influenced by substrates in which the cell attached. Cells on crosslinked substrate show an uneven distribution of cell cycle with an IC_{50} of 5.46 nM. On the other hand, cells on non-crosslinked P(CL-*co*-DLLA) substrate shows an accumulation of G0/G1 phase and controlled release of S and G2/M phase with an IC_{50} of paclitaxel is 2.86 nM. Thus, the fluidity-tunable PCL-based substrate is considered as a novel material to control the behavior of cancer cells for various biomedical applications.

5. Conclusion

We demonstrate the influence of crosslinked and non-crosslinked P(CL-*co*-DLLA) substrates on cancer cell behaviors such as cell morphology, focal adhesion, proliferation, apoptosis, cell cycle and anti-cancer drug activity. Cancer cell shows a diverse type of behavior on crosslinked and non-crosslinked substrates. Cells on crosslinked substrate show well-spread actin stress fibers, increased proliferation rate with an active S phase. However, cells on non-crosslinked substrate show rounded morphology, decreased proliferation with an accumulated G0/G1 phase. NCI-H232 cells on non-crosslinked substrate show a controlled release of the cell cycle through a G0/G1 phase to G2/M phase. IC_{50} of paclitaxel for cells on crosslinked and non-crosslinked substrates has noticed that 5.46 nM and 2.86 nM, respectively. This suggests that IC_{50} of anti-cancer drug paclitaxel for NCI-H23 cells on PCL substrates depends on the growth profile of cells. From the above findings, our PCL-based crosslinked and non-crosslinked substrates are considered as a novel technique to regulate the growth and behavior of cancer cells. This study will provide necessary information regarding the application of fluidic, biodegradable PCL-based substrates for in vivo models for cancer therapy.

Conflict of Interest

The authors declare that there is no conflict of interests.

References

1. Nishimura N, Sasaki T (2008) Regulation of epithelial cell adhesion and repulsion: role of endocytic recycling. *J Med Invest* 55: 9–15.
2. Sheetz MP, Felsenfeld DP, Galbraith CG (1998) Cell migration: regulation of force on extracellular-matrix-integrin complexes. *Trends Cell Biol* 8: 51–54.
3. Koohestani F, Braundmeier AG, Mahdian A, et al. (2013) Extracellular matrix collagen alters cell proliferation and cell cycle progression of human uterine leiomyoma smooth muscle cells. *PLOS ONE* 8: e75844.

4. Philp D, Chen SS, Fitzgerald W, et al. (2005) Complex extracellular matrices promote tissue-specific stem cell differentiation. *Stem Cells* 23: 288–296.
5. Farrelly N, Lee YJ, Oliver J, et al. (1999) Extracellular matrix regulates apoptosis in mammary epithelium through a control on insulin signaling. *J Cell Biol* 144: 1337–1347.
6. Lu P, Weaver VM, Werb Z (2012) The extracellular matrix: a dynamic niche in cancer progression. *J Cell Biol* 196: 395–406.
7. Pickup MW, Mouw JK, Weaver VM (2014) The extracellular matrix modulates the hallmarks of cancer. *EMBO Reports* 15: 1243–1253.
8. Ulrich TA, Pardo EMDJ, Kumar S (2009) The mechanical rigidity of the extracellular matrix regulates the structure, motility, and proliferation of glioma cells. *Cancer Res* 69: 4167–74.
9. Yeung T, Georges PC, Flanagan LA, et al. (2005) Effects of substrate stiffness on cell morphology, cytoskeletal structure, and adhesion. *Cell Motil Cytoskel* 60: 24–34.
10. Tilghman WR, Blais EM, Cowan CR, et al. (2012) Matrix rigidity regulates cancer cell growth by modulating cellular metabolism and protein synthesis. *PLOS ONE* 7: e37231.
11. Pathak A, Kumar S (2012) Independent regulation of tumor cell migration by matrix stiffness and confinement. *Proc Natl Acad Sci U S A* 109: 10334–10339
12. Liu J, Tan Y, Zhang H, et al. (2012) Soft fibrin gels promote selection and growth of tumorigenic cells. *Nat Mat* 11: 734–741.
13. Ghosh K, Ingber DE (2007) Micromechanical control of cell and tissue development: Implications for tissue engineering. *Advan Drug Deliv Rev* 59: 1306–1318.
14. Eshraghi S, Das S (2012) Micromechanical finite element modeling and experimental characterization of the compressive mechanical properties of polycaprolactone: hydroxyapatite composite scaffolds prepared by selective laser sintering for bone tissue engineering. *Acta Biomater* 8: 3138–3143.
15. Duncan R (2003) The dawning era of polymer therapeutics. *Nat Rev Drug Discov* 2: 347−360.
16. Peer D, Karp JM, Hong S, et al. (2007) Nanocarriers as an emerging platform for cancer therapy. Nat *Nanotech* 2: 751–760.
17. Krishnan V, Xu X, Barwe SP, et al. (2013) Dexamethasone-loaded block copolymer nanoparticles induce leukemia cell death and enhance therapeutic efficacy: A novel application in pediatric nanomedicine. *Mol Pharmaceutics* 10: 2199−2210.
18. Pathak A, Kumar S (2013) Dual anticancer drug/superparamagnetic iron oxide-loaded PLGA-based nanoparticles for cancer therapy and magnetic resonance imaging. *Int J Pharm* 447: 94–101.
19. Woodruff MA, Hutmacher DW (2010) The return of a forgotten polymer: Polycaprolactone in the 21st century. *Progress in Polymer Sci* 35: 1217–1256.
20. Abedalwafa M, Wang F, Wang L, et al. (2013) Biodegradable poly-epsilon-caprolactone (PCL) for tissue engineering applications: a review. *Rev Adv Mater Sci* 34: 123–140.
21. Rie JV, Declercq H, Hoorick JV, et al. (2015) Cryogel-PCL combination scaffolds for bone tissue repair. *J Mater Sci Mater Med* 26:123.
22. Uto K, Muroya T, Okamoto M, et al. (2012) Design of super-elastic biodegradable scaffolds with longitudinally oriented microchannels and optimization of the channel size for schwann cell migration. *Sci Technol Adv Mater* 13: 064207.

23. Uto K, Yamamoto K, Hirase S, et al. (2006) Temperature-responsive cross-linked poly(ε-caprolactone) membrane that functions near body temperature. *J Control Release* 110: 408–413.
24. Ebara M, Uto K, Idota N, et al. (2012) Shape-memory surface with dynamically tunable nano-geometry activated by body heat. *Adv Mater* 24: 273–278.
25. Versaevel M, Grevesse T, Gabriele S (2012) Spatial coordination between cell and nuclear shape within micropatterned endothelial cells. *Nat Commun* 3: 671.
26. Forte G, Pagliari S, Ebara M, et al. (2012) Substrate stiffness modulates gene expression and phenotype in neonatal cardiomyocytes in vitro. *Tissue Eng Part A* 18: 1837–1848.
27. Romanazzo S, Forte G, Ebara M, et al. (2012) Substrate stiffness affects skeletal myoblast differentiation in vitro. *Sci Technol Adv Mater* 13: 064211.
28. Uto K, Ebara M, Aoyagi T (2014) Temperature-responsive poly(ε-caprolactone) cell culture platform with dynamically tunable nano-roughness and elasticity for control of myoblast morphology. *Int J Mol Sci* 15: 1511–1524.
29. Sell SA, Wolfe PS, Garg K (2010) The use of natural polymers in tissue engineering: a focus on electrospun extracellular matrix analogues. *Polymers* 2: 522–553.
30. Gunatillake PA, Adhikari R (2003) Biodegradable synthetic polymers for tissue engineering. *European Cells and Mat* 5: 1–16.
31. Breuls RGM, Jiya TU, Smit TH (2008) Scaffold stiffness influences cell behavior: opportunities for skeletal tissue engineering. *Open Orthopedics* 2: 103–109.
32. Park JS, Chu JS, Tsou AD (2011) The effect of matrix stiffness on the differentiation of mesenchymal stem cells in response to TGF-b. *Biomaterials* 32: 3921–3930.
33. Ni Y, Chiang MYM (2007) Cell morphology and migration linked to substrate rigidity. *Soft Matter* 3: 1285–1292.
34. Yeung T, Georges PC, Flanagan LA (2005) Effects of substrate stiffness on cell morphology, cytoskeletal structure, and adhesion. *Cell Motil Cytoskeleton* 60: 24–34.
35. Tilghman RW, Cowan CR, Mih JD, et al. (2010) Matrix rigidity regulates cancer cell growth and cellular phenotype. *PLOS ONE* 5: 9.
36. Wozniak MA, Modzelewska K, Kwong L, et al. (2004) Focal adhesion regulation of cell behavior. *Biochim Biophys Acta* 1692: 103–119.
37. Kroemer G, Galluzzi L, Vandenabeele P, et al. (2009) Classification of cell death: recommendations of the nomenclature committee on cell death. *Cell Death Differ* 16: 3–11.
38. Campisi J, Fagagna FDD (2007) Cellular senescence: when bad things happen to good cells. *Nat Rev Mol Cell Biol* 8: 729–740.
39. Chen QM, Liu J, Merrett JB (2000) Apoptosis or senescence-like growth arrest: influence of cell-cycle position, p53, p21 and bax in H_2O_2 response of normal human fibroblasts. *Biochem J* 15: 543–551.
40. Assoian RK, Klein EA (2008) Growth control by intracellular tension and extracellular stiffness. *Trends Cell Biol* 18: 347–352.
41. Vicencio JM, Galluzzi L, Tajeddine N, et al. (2008) Senescence, apoptosis or autophagy? when a damaged cell must decide its path- A mini review. *Gerontology* 54: 92–99.
42. Johnson DG, Walker CL (1999) Cyclins and cell cycle checkpoints. *Annu Rev Pharm Tox* 39: 295–312.

43. Davis PK, Ho A, Dowdy SF (2001) Biological methods for cell-cycle synchronization of mammalian cells. *Bio Techniques* 30: 1322–1331.
44. Tian Y, Luo C, Lu Y, et al. (2012) Cell cycle synchronization by nutrient modulation, *Integr Biol (Camb)* 4: 328–334.
45. Lee WC, Bhagat AAS, Huang S, et al. (2011) High-throughput cell cycle synchronization using inertial forces in spiral microchannels. *Lab Chip* 11: 1359–1367.
46. Chen M, Huang J, Yang X, et al. (2012) Serum starvation induced cell cycle synchronization facilitates human somatic cells reprogramming. *PLOS ONE* 7: e28203.
47. Gstraunthaler G (2003) Alternatives to the use of fetal bovine serum: Serum-free cell culture, *ALTEX* 20: 275–281.
48. Eric AK, Liqun Y, Devashish K, et al. (2009) Cell-cycle control by physiological matrix elasticity and in vivo tissue stiffening. *Curr Biol* 19: 1511–1518.
49. Özdemir O (2011) Negative impact of paclitaxel crystallization on hydrogels and novel approaches for anticancer drug delivery systems, Current cancer treatment- Novel beyond conventional approaches. *In Tech Open, Croatia* 767–782
50. Chiang PC, Goul S, Nannini M (2014) Nanosuspension delivery of paclitaxel to xenograft mice can alter drug disposition and anti-tumor activity. *Nanoscale Res Lett* 9: 156.
51. Liebmann JE, Cook JA, Lipschultz C, et al. (1993) Cytotoxic studies of pacfitaxel (Taxol®) in human tumour cell lines. *Br J Cancer* 68: 1104–1109.

AIMS Press